Purified Human MDR 1 Modulates Membrane Potential in Reconstituted Proteoliposomes†

Ellen M. Howard and Paul D. Roepe*

Department of Chemistry, Department of Biochemistry and Molecular Biology, and Lombardi Cancer Center Program in Tumor Biology, Georgetown University, 37th and O Streets, Washington, D.C. 20057

Received August 22, 2002; Revised Manuscript Received November 14, 2002

ABSTRACT: Human multidrug resistance (hu MDR 1) cDNA was fused to a *P. shermanii* transcarboxylase biotin acceptor domain (TCBD), and the fusion protein was heterologously overexpressed at high yield in K^+-uptake deficient *Saccharomyces cerevisiae* yeast strain 9.3, purified by avidin−biotin chromatography, and reconstituted into proteoliposomes (PLs) formed with *Escherichia coli* lipid. As measured by pH- dependent ATPase activity, purified, reconstituted, biotinylated MDR−TCBD protein is fully functional. Dodecyl maltoside proved to be the most effective detergent for the membrane solubilization of MDR−TCBD, and various salts were found to significantly affect reconstitution into PLs. After extensive analysis, we find that purified reconstituted MDR−TCBD protein does not catalyze measurable H^+ pumping in the presence of ATP. In the presence of physiologic [ATP], K^+/Na^+ diffusion potentials monitored by either anionic oxonol or cationic carbocyanine are easily established upon addition of valinomycin to either control or MDR−TCBD PLs. However, in the absence of ATP, although control PLs still maintain easily measurable K^+/Na^+ diffusion potentials upon addition of valinomycin, MDR−TCBD PLs do not. Dissipation of potential by MDR−TCBD is clearly [ATP] dependent and also appears to be Cl^- dependent, since replacing Cl^- with equimolar glutamate restores the ability of MDR−TCBD PLs to form a membrane potential in the absence of physiologic [ATP]. The data are difficult to reconcile with models that might propose ATP-catalyzed "pumping" of the fluorescent probes we use and are more consistent with electrically passive anion transport via MDR−TCBD protein, but only at low [ATP]. These observations may help to resolve the confusing array of data related to putative ion transport by hu MDR 1 protein.

The 170 kDa human multidrug resistance protein (hu MDR 1 or p-glycoprotein, p-gp)[1] has been studied extensively for over 15 years. It is localized predominantly to the plasma membrane of a variety of cell types and is homologous to other ATP-binding cassette (ABC) proteins such as the cystic fibrosis transmembrane conductance regulator (CFTR) and sulfonyl urea receptor (SUR) ion channels. The normal physiological function of hu MDR 1 has not yet been fully determined, but some clues are gathered by noting that the highest endogenous expression of the protein is typically within polarized epithelia. When any of a variety of cell types are selected with any of a variety of cytotoxic compounds, or exposed to radiation, differentiation agents, and/or other forms of stress, hu MDR 1 protein is frequently overexpressed. Cells overexpressing the protein are typically resistant to the selecting agent or treatment and also typically exhibit cross-resistance to a wide variety of cytotoxic drugs and other forms of stress including withdrawal of growth factors (*1*) and complement-mediated cytotoxicity (*2*, *3*). Transfection of hu MDR 1 cDNA without any drug selection of resultant clones confers variable levels of resistance to drugs or cytotoxic stress (*4*, *5*) that (depending on the drug) is frequently lower than that observed in drug-selected or drug-conditioned cell lines.

It is likely that hu MDR 1 protein acts as a transporter, and many investigators have suggested that there may be several classes of transported substrates and even multiple thermodynamic and kinetic modes of transport (*6*). A frequently championed model for hu MDR 1 function is that it acts as an ATP-dependent nonspecific drug pump that expels a plethora of hydrophobic compounds from inside the cell and/or the cell plasma membrane to outside the cell. This model has been challenged since net outward movement of any putative substrate by hu MDR 1 protein (against a substrate gradient and with a rate constant faster than that of substrate passive diffusion) has never been unequivocally observed and because the energetics of such a process would be extremely surprising (*7*). Another model is that the protein flips one or more lipids between membrane leaflets (*8*), and a third is that it performs some type of ion transport (*9*, *10*). Early suggestions that the protein catalyzes Cl^- transport, possibly as a volume-regulated Cl^- channel, proved highly

† E.M.H. was a Clare Boothe Luce Fellow during the course of this work.

* To whom correspondence should be addressed. Telephone: (202) 687-7300. Fax: (202) 687-6209. E-mail: roepep@georgetown.edu.

[1] Abbreviations: MDR, multidrug resistance; TCBD, transcarboxylase biotin acceptor domain; PLs, proteoliposomes; p-gp, p-glycoprotein; ABC, ATP-binding cassette; CFTR, cystic fibrosis transmembrane conductance regulator; SUR, sulfonyl urea receptor; $\Delta\Psi$, membrane potential; $DiOC_5(3)$, 3,3′-dipentyloxacarbocyanine iodide; $DiSBAC_2(3)$, bisoxonol or bis(1,3-diethylthiobarbituric acid)trimethine oxonol; LPC, lysophosphatidylcholine; DM, dodecyl maltoside; SC-ura, synthetic complete media lacking uracil; SUV, small unilammelar vesicles; ISOVs, inside-out plasma membrane vesicles; OG, octyl β-glucoside; AO, acridine orange; VPL, verapamil.

10.1021/bi026706i CCC: $25.00
Published on Web 03/08/2003

controversial. A variety of studies were reported using widely different cell systems (many reviewed in ref *9*), leading to a series of revised ion transport models that culminated in the general idea that hu MDR 1 may either (1) regulate endogenous cell volume-regulated Cl^- channels or (2) be a phosphorylation- and ATP-dependent Cl^- channel. Regardless, in whatever form, this putative ion transport function could in theory confer resistance to various forms of stress (drugs, immunological agents, induction of apoptosis, etc.) because when hu MDR 1 is overexpressed it would then perturb normal maintenance of cellular and subcellular volume, pH, and/or membrane potential (*11*), as well as various signaling pathways that are controlled in part by ion transport (*1*). The magnitude and regulation of pH gradients and electrical membrane potentials across various cell membranes control passive diffusion and accumulation of amphipathic drugs, are involved in regulating assembly of pores necessary for complement-mediated cytotoxicity (*3*), and are involved in the signaling associated with induction of apoptosis (*1, 12*).

In general support of the ion transport models, LR73 cells stably transfected with hu MDR 1 cDNA were found to exhibit a more alkaline cytosolic pH and decreased electrical membrane potential ($\Delta\Psi$) (*4*) and to perform unusual Cl^- gradient-dependent H^+ transport (*10*). However, another recent study observed that hu MDR 1 protein overexpression did not alter $\Delta\Psi$ in MCF7 cells but might alter the intramembraneous dipole potential (*5*). Along with earlier conflicting data both in support of and arguing against Cl^- channel function of hu MDR 1 protein (reviewed in ref *9*), it is therefore currently unclear exactly what type of ion transport hu MDR 1 protein might perform, under what conditions this might occur, and how this might effect $\Delta\Psi$ and ΔpH. Much of the complexity in interpretation arises from the fact that many of the studied systems have been mammalian cells that are not true transfectants but are rather cells selected for overexpression of hu MDR 1 via exposure to various cytotoxic drugs. We now know that there are many alterations in these cells that are due to drug selection conditions but not to MDR protein and that these greatly complicate analysis (*7*).

Thus, several groups have purified hu MDR 1 protein from various cell types including yeast (*13*−*17*) with the obvious goal of better defining molecular level function in a system of reduced complexity. However, to our knowledge, no laboratories have yet performed ion transport studies with purified reconstituted systems. Several groups have heterologously expressed MDR genes fused to a polyhistidine codon tag and have purified the fusion proteins via Ni^{2+} chelation chromatography (*14*, *18*, *19*). Recently, Gros and colleagues combined this approach with the addition of a biotin acceptor domain to mouse mdr3 protein (*13*) and purified it with two-step Ni^{2+} chelation and streptavidin affinity chromatography. As far as we are aware, no laboratories have published purification of heterologously expressed MDR protein from yeast in the absence of the reducing conditions associated with Ni^{2+} chelation chromatography.

Data obtained with these purified preparations have defined drug, pH, and lipid phase effects on the ATPase activity of hu MDR 1 and provide a wide range of observed catalytic activity [0.11−2.1 μmol of P_i (mg of hu MDR 1)$^{-1}$ min^{-1}]. There have also been a few reports of drug transport measured with purified reconstituted MDR proteins, but these do not in general control for altered passive transport due to possible electrochemical driving forces or volume effects.

For these reasons, we have purified a biotin acceptor domain−hu MDR 1 fusion protein without using Ni^{2+} chelation chromatography, have reconstituted the protein into proteoliposomes, and have analyzed the ion transport properties of these preparations using pH and $\Delta\Psi$ responsive probes.

MATERIALS AND METHODS

Materials. The anti hu MDR 1 C219 monoclonal antibody was from Signet Laboratories. Streptavidin−HRP, biotinylated molecular weight markers, and ECL detection reagents were from Amersham. Immobilized monomeric avidin resin was from Pierce. Yeast and bacteria growth media components were from Difco. Oligonucleotides were custom synthesized by Gibco-BRL. Nigericin, valinomycin, bis-(1,3-diethylthiobarbituric acid)trimethine oxonol [bisoxonol, $DiSBAC_2(3)$], 3,3′-dipentyloxacarbocyanine iodide [$DiOC_5(3)$], and bis(3-phenyl-5-oxoisoxazol-4-yl)pentamethine oxonol (oxonol V) were from Molecular Probes. Purified *Escherichia coli* lipid extract and lysophosphatidylcholine (LPC) were from Avanti Polar Lipids. Dodecyl maltoside (DM) was from Calbiochem. All other reagents were of reagent grade or better and were purchased from Sigma.

Bacterial Strain. The *E. coli* strain NM522 [*hsd* Δ *5* Δ *(lac-pro)F*$^-$ *lacI lacZ* Δ*M15 pro supE*] was used in all bacterial work.

Construction of Plasmid pYKMDRBio6. A 3′ 494 bp fragment of the 4.3 kbp hu MDR 1 cDNA and a 346 bp *P. shermanii* transcarboxylase biotin acceptor domain (TCBD) cDNA fragment were PCR amplified from pYKM77 (kindly provided by Drs. K. Kuchler and J. Thorner, University of California, Berkeley) and YEp352/BIO6 (kindly provided by Dr. A. Tzagoloff, Columbia University), respectively. Oligonucleotides were designed to be complementary to both the stop codon region of hu MDR 1 cDNA and the 5′ end of the relevant fragment of TCBD cDNA. The MDR 5′ primer sequence (5′) TCC TGT TTG A**CT GCA G**CA TTG CTG AG (3′) was complementary to hu MDR 1 cDNA near a *Pst*I site (in bold). The MDR 3′ primer sequence (5′) GAG CTC G<u>AA GCT TC</u>*G CGG CCG C*TT TGT TCC AGC CTG <u>GAC AAT G</u> (3′) destroyed the stop codon, included additional nucleotides complementary to the 5′ end of the TCBD fragment, and contained *Hin*dIII (underlined) and engineered *Not*I (in italics) restriction sites. The TCBD 5′ primer sequence (5′) AAA *GCG GCC GC*G AGG CTT CGA GCT CGG TAC CCG GGG ATC C (3′) included a 5′ tail fully complementary to the MDR fragment, and the TCBD 3′ primer sequence (5′) GGC CAG TGC C<u>AA GCT T</u>GC ATG CTT GCA GGT (3′) destroyed an endogenous *Pst*I site, but a *Hin*dIII site (underlined) was retained. Isolated plasmids pYKM77 and YEp352/BIO6 were PCR amplified individually, and the fragments were then gel purified, combined to act as template, and PCR amplified in the presence of excess MDR 5′ and TCBD 3′ primers. The resultant in-frame 807 bp gene fusion was trimmed with *Pst*I and *Hin*dIII, inserted into partially digested pYKM77, and transformed into *E. coli* NM522, and the recombinant plasmid was colony purified. The resultant construct encodes

full-length hu MDR 1 protein fused in-frame (at the very C terminus) to an efficient 83 amino acid biotin acceptor domain (TCBD).

Yeast Strains and Growth Conditions. Saccharomyces cerevisiae 9.3 (*Mat a leu2 ura3 trp1 ade2 trk1Δ trk2Δ ena1::His3::ena4*) was kindly provided by Dr. Alonso Rodriguez-Navarro, Universidad Politechnica, Madrid, Spain. 9.3 yeast harboring pYKM77, pYKMDRBio6, or pVT101 were selected for growth in synthetic complete media lacking uracil (SC-ura) supplemented with 100 mM KCl.

Preparation of Yeast Plasma Membranes. The acid precipitation method of Goffeau and Dufour (*20*) with some modifications (*21*) was used to purify yeast plasma membranes.

Purification and Reconstitution of Biotinylated MDR Protein. Purified plasma membranes from 9.3 harboring pYKMDRBio6 were resuspended to a protein concentration of 1 mg/mL in solubilization buffer [0.75% DM/500 mM NaCl/50 mM Tris-HCl, pH 7.5/250 mM sucrose/20% (v/v) glycerol/1 mM MgATP/1 mM $MgCl_2$/6.5 mM DTT] and mixed gently for 1 h at 4 °C. The unsolubilized material was removed by centrifugation (100000*g*, 1 h, 4 °C). DM extracts were loaded on immobilized monomeric avidin resin which had been preequilibrated in column wash buffer [0.1% DM/250 mM NaCl/50 mM Tris-HCl, pH 7.5/250 mM sucrose/20% (v/v) glycerol/1 mM $MgCl_2$/6.5 mM DTT]. The column was washed with 6 bed volumes of column wash buffer, and biotinylated MDR protein (MDR−TCBD) was eluted with 5 mL of elution buffer (2 mM D-biotin in the column wash buffer). Purified protein was pooled and reconstituted by first incubating the column fractions with 1.4% *E. coli* total lipid extract for 30 min on ice. The protein/detergent/lipid mixture was then dialyzed overnight against 500 volumes of dialysis buffer [10 mM Tris, pH 7.5/70 mM sucrose/1 mM DTT/1 mM EDTA/140 mM salt (salt was varied for different preparations; see Results)]. If necessary, [salt] was decreased and [sucrose] was increased to maintain osmotic balance. The protein/lipid mixture was centrifuged (200000*g*, 1 h, 4 °C), and proteoliposomes (PLs) were resuspended in dialysis buffer, snap frozen in dry ice/ethanol, and stored at −80 °C. Before use in activity assays, the PLs were sonicated for exactly 7 s in a Racker bath sonifier. From 10 mg of purified plasma membrane protein, we regularly obtained approximately 100 μg of purified MDR−TCBD protein. Control PLs were made in identical fashion, but with column fractions not containing eluted MDR−TCBD combined with lipid instead of fractions harboring eluted MDR−TCBD. Western blot with the monoclonal antibody C219 verified that control PLs did not contain MDR−TCBD.

ATPase Activity Assays. The ATP-dependent release of inorganic phosphate was measured using the method of Chifflet et al. (*22*) with some modifications (*21*). When the protein was in detergent/lipid solutions, these were included in background experiments to control for any artifacts from the detergent or lipid.

Transport Assays. Transport experiments were performed in 3 mL methacrylate disposable cuvettes in a PTI Alphascan fluorometer. The temperature was maintained at 37 °C using a water-jacketed cuvette holder. To measure changes in pH, a previously described acridine orange (AO) based assay was employed (*21*). Transport buffer was adjusted to preserve isotonicity as required (see Results).

For experiments using the lipophilic cation 3,3′-dipentyloxacarbocyanine iodide [$DiOC_5(3)$], the excitation and emission wavelengths were 475 and 496 nm, respectively. PLs were diluted into transport buffer [10 mM Tris, pH 7.5/70 mM sucrose/1 mM EDTA/1 mM DTT/4 mM $MgCl_2$ ($MgSO_4$ for Cl^--free experiments)/140 mM salt] in the presence or absence of Mg^{2+}-ATP and 100 nM $DiOC_5(3)$ (see Results). After equilibration for 500 s, typically, 7 μM valinomycin was added followed by 1.5 μM gramicidin D at 1000 s (see Results).

We also calibrated membrane potential more precisely using oxonol V, the predictions of the Nernst equation, and adapting a method previously described for small unilammelar vesicles (SUVs) harboring purified K^+ channel protein (*23*). PLs with high K^+ inside (140 mM KCl) were equilibrated in buffer containing high Na^+ and low K^+ (126 mM NaCl/14 mM KCl) with 8 μM oxonol V in the presence and absence of 1 μM valinomycin and/or ±2 mM ATP. When valinomycin is present, the $\Delta\Psi$ is clamped at −60 mV (see Results). By including additional KCl in the medium, $\Delta\Psi$ is clamped to different values and can be calibrated by measuring the fluorescence response of oxonol V(see Results and ref *23*).

RESULTS

Expression and Purification of the hu MDR−TCBD Fusion Protein. We fused a transcarboxylase biotin acceptor domain (TCBD) to the carboxyl terminus of hu MDR 1 and purified detergent-extracted fusion protein via streptavidin affinity chromatography (Figure 1). The addition of the TCBD increased the mass of hu MDR 1 protein by 12 kDa, and biotinylated MDR−TCBD protein was easily detected in the plasma membrane of *S. cerevisiae* using HRP-conjugated streptavidin (Figure 1A). High levels of biotinylated MDR−TCBD migrating near 155 kDa were detected in strain 9.3 plasma membranes whereas the native hu MDR 1 protein expressed in yeast migrates near 140 kDa (*21*). A variety of detergent conditions were attempted, and we found that hu MDR−TCBD protein was almost completely and yet selectively solubilized with DM in the presence of 500 mM NaCl (lanes 2, Figure 1A,B). The DM extract was loaded onto monomeric avidin and eluted with 2 mM D-biotin (see Materials and Methods). Some MDR−TCBD protein that was not efficiently biotinylated *in vivo* did not adhere to the column since an immunoreactive (but not well biotinylated) band was detected in the flow-through fraction (lane 3, Figure 1A vs 1B). MDR−TCBD was eluted with free biotin and was reconstituted in *E. coli* lipid extract via slight modifications to a previously reported dialysis method (*16*). Silver-stained SDS−PAGE revealed that the heterologously expressed MDR−TCBD protein was purified at least 1000-fold via this protocol (Figure 1C).

While optimizing conditions for purification, we noticed some intriguing effects of detergent solubilization. For example, although octyl β-glucoside (OG) proved the most effective detergent for solubilizing native hu MDR 1 protein from 9.3 yeast membranes, it proved much less effective for the MDR−TCBD fusion protein (data not shown). MDR−TCBD was nearly completely solubilized by DM plus >250 mM NaCl, similar to previous observations (*14*).

Reconstitution of MDR−TCBD. To examine ion transport with reconstituted MDR−TCBD PLs, we first examined

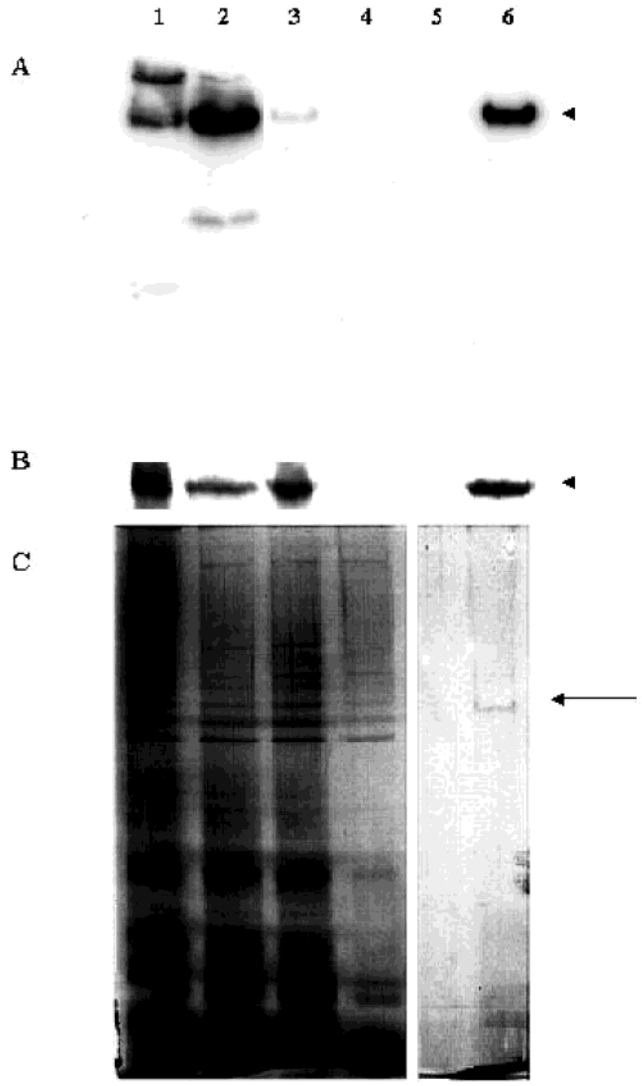

FIGURE 1: Expression and purification of biotinylated hu MDR 1 (MDR−TCBD) protein. (A) Biotin detection blot using streptavidin−HRP: (lane 1) 100 μg of 9.3/MDR−TCBD plasma membrane protein; (lane 2) 50 μg of DM solubilized extract from 9.3/MDR−TCBD plasma membranes; (lane 3) 25 μg of protein flow-through from the monomeric avidin column during solubilized extract application; (lane 4) 10 μg of protein washed from the column with column wash buffer after sample application; (lane 5) column wash buffer; (lane 6) 2 μg of protein eluted with 2 mM D-biotin. The arrow indicates 150−155 kDa; in yeast, hu MDR 1 protein is not glycosylated, migrating at a molecular mass of 140 kDa (*21*), but the addition of the TCBD increases the mass to 155 kDa. (B) The biotin blot in (A) was stripped and reprobed with mouse monoclonal antibody C219 and anti-mouse IgG−HRP. Note that in lane 3 vs lane 2 the immunoreactive band is more intense in the western blot relative to the ratio seen in the biotin blot. This is because all MDR−TCBD is not biotinylated *in vivo*, the nonbiotinylated protein does not adhere to the column, and the biotinylated species adheres very well. (C) Silver-stained SDS−PAGE. The lanes correspond to the same samples as in (A) and (B). However, lanes 1−4 contain 5 μg of protein each, and lane 6 contains 1 μg of protein. Lanes 5 and 6 were run with the other four lanes on the same gel but were separated from the rest of the gel and developed for 20 min rather than 5 min.

reconstitution in the presence of various salts to verify that ion concentration inside the PLs could be manipulated without severely compromising MDR−TCBD:lipid ratios in the reconstituted PLs. Thus, purified MDR−TCBD was mixed with purified *E. coli* lipid and the mixture dialyzed

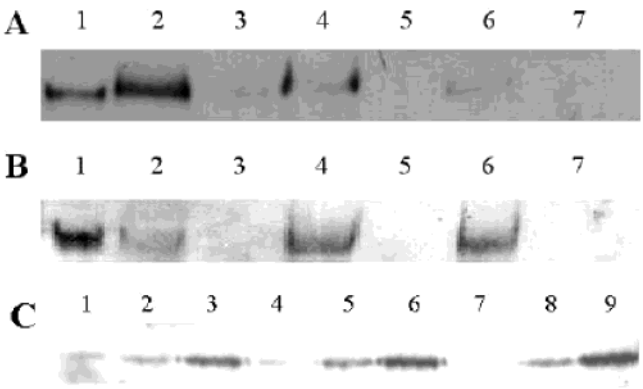

FIGURE 2: Reconstitution of MDR−TCBD. Purified MDR−TCBD protein was reconstituted into PLs via dialysis in the presence of different salts, PLs were collected, approximately 2.5 μg of lipid was loaded per lane, and streptavidin−HRP detection revealed the level of purified MDR−TCBD associated to lipid in each sample. (A) Samples reconstituted with K^+ salts. (B) Samples reconstituted with Na^+ salts. Lanes: (1) 2 μg of unreconstituted MDR−TCBD protein eluted from the monomeric avidin resin; (2, 4, 6) MDR−TCBD PLs in the presence of 140 mM Cl^- (i.e., lane 2 in panel A is KCl, lane 2 in panel B is NaCl), 140 mM glutamate$^-$, 140 mM acetate$^-$, respectively; (3, 5, 7) similarly treated negative control PLs (no MDR−TCBD) formed in the presence of the same salts, respectively. (C) The orientation of MDR−TCBD in sonified PLs was determined by incubating MDR−TCBD PLs with monomeric avidin resin in the presence of 0 (lanes 1−3), 0.1% (lanes 4−6), or 1.0% (lanes 7−9) DM and detecting MDR−TCBD in various fractions via streptavidin−HRP. The avidin beads were centrifuged, and the supernatant was collected (unbound MDR−TCBD PLs, lanes 1, 4, and 7), the beads were washed with the same buffer and recentrifuged, and the wash was collected (lanes 2, 5, and 8), and the beads were then eluted with 2 mM D-biotin and recentrifuged, and supernatants were collected once again (lanes 3, 6, and 9).

against buffer of various salt compositions, keeping all other factors (i.e., pH, volume, time) constant, and the efficiency of incorporation was then determined by HRP−streptavidin detection of MDR−TCBD within a fixed amount of lipid in the collected PLs (Figure 2). When we varied diazylate salt composition to incorporate different salts inside the PLs, we noticed that reconstitution was salt dependent (Figure 2). For example, while KCl was the most effective of the K^+ salts examined (Figure 2, lane A2), NaCl was the least effective of the Na^+ salts examined (Figure 2, lane B2) and did not yield levels of incorporated MDR−TCBD comparable to those achieved with KCl.

Prior to functional analysis, it was important to determine the orientation of MDR−TCBD in PLs. Taking advantage of the TCBD, PLs formed by sonification for 7 s in a Racker bath sonifier were incubated with monomeric avidin beads in the presence of 0, 0.1%, or 1.0% DM (Figure 2C). The beads were centrifuged, washed with incubation buffer, and then eluted with D-biotin. PLs with MDR−TCBD in the inside-out orientation relative to the cell plasma membrane adhere to the avidin resin in the absence of detergent (Figure 2C, lanes 1−3). At 1.0% concentration, DM partially solubilizes the PLs, allowing additional MDR−TCBD that is in the right-side-out orientation to also bind to the monomeric avidin beads; thus, in the presence of 1% DM all MDR−TCBD adheres to the monomeric avidin as expected (Figure 2C, lanes 7−9). The majority of MDR−TCBD adhered to the resin in the absence of detergent and was specifically eluted with D-biotin (Figure 2C, lanes 1−3),

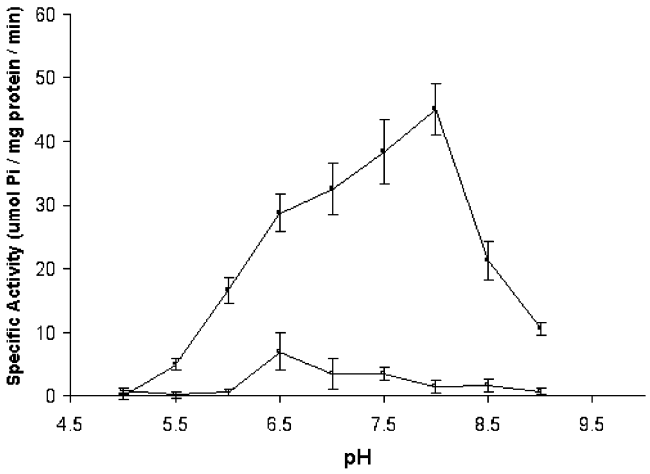

FIGURE 3: pH-dependent ATPase activity of reconstituted MDR−TCBD PLs. The vanadate-inhibitable ATP-dependent release of P_i was measured over a range of pH (5.0−9.0) for MDR−TCBD PLs (top) and compared to purified 9.3/MDR−TCBD plasma membranes (bottom). Reported is the average of six experiments from two different preparations in each case ± the standard error. The pH profile for purified, reconstituted protein is similar to data reported previously and actually corresponds to among the highest specific activity yet recorded (see text). Depending on pH, most of the plasma membrane ATPase activity is due to the endogenous plasma membrane ATPase (PMA1), with an estimated 5% due to MDR−TCBD in these membranes at pH 6.5−7.0. If specific activities are ratioed, and this conservative estimate is used, the fold enrichment in MDR−TCBD ATPase activity is at least 300- and 600-fold at pH 7.0−8.0. Based on western blot intensities (Figure 1) our fold purification is nearer 1000-fold.

showing that the biotin acceptor domain (hence the C terminus and ATP hydrolysis domains) was oriented predominately on the outside surface of the PL. Preincubation of hu MDR 1−TCBD PLs with free avidin in the absence of detergent abolished binding of the PLs to the avidin beads (not shown). After densitometry of Figure 2C we calculate that approximately 75% of the protein is oriented inside out (see also ATPase activity data below).

ATPase Activity of Purified, Reconstituted MDR−TCBD. To test whether reconstituted MDR−TCBD protein was fully functional, and to further test orientation, we measured pH-dependent, vanadate-inhibitable ATPase activity (Figure 3). The specific activity at pH 7.5 was 3.83 ± 0.9 and 0.331 ± 0.13 μmol of P_i (mg of protein)$^{-1}$ min^{-1} for MDR−TCBD PLs and 9.3/MDR−TCBD plasma membranes (which contain both MDR−TCBD and endogenous yeast ATPases), respectively. Since only (at most) 5% of the yeast plasma membrane ATPase activity at pH 7.5 can be attributed to MDR−TCBD, by this approximate measure purification enhanced the specific activity of MDR−TCBD by (at least) 300−600-fold. Calculating fold purification via integrating the intensity of immunoreactivity vs total protein applied to a western gel (Figure 1C) yields approximately 1000-fold purification. The pH profile of purified MDR protein ATPase activity (Figure 3) is consistent with previous results (*16*), and the specific activity we measure is on the high end of the range of values previously reported in the literature (see Figure 3 caption). Other purified hu MDR 1 protein preparations are reported to have a specific activity of 0.11−2.1 μmol of P_i (mg of protein)$^{-1}$ min^{-1} (e.g., refs *15*, *16*, *19*, *24*, and *25*). Thus, our reconstituted MDR−TCBD preparations are highly purified and, to the best of our ability to ascertain, retain full ATPase activity.

Is hu MDR 1 Protein a H^+-ATPase? Previous experiments from our laboratory with LR73/hu MDR 1 transfectants (*4*) and yeast inside-out plasma membrane vesicles (ISOVs) harboring hu MDR 1 protein (*21*, *26*) were consistent with hu MDR 1 performing H^+ transport either directly (e.g., as some type of active H^+ transporter) or indirectly (e.g., via influencing membrane potential or volume that then secondarily affected H^+ transport). Under a variety of conditions, we extensively tested whether reconstituted MDR−TCBD PLs performed direct ATP-driven H^+ transport, but we never observed formation of a measurable ΔpH (Figure 4).

MDR−TCBD Collapses Diffusion Potential in Reconstituted PLs. If PLs are formed in the presence of KCl and at a given pH and then diluted into equimolar NaCl at the same pH, a K^+/Na^+ diffusion potential across the PL membranes (negative inside) should be generated upon the addition of the K^+-specific ionophore valinomycin. This is because internal K^+ diffuses out (down the chemical concentration gradient) via valinomycin, but Na^+ and Cl^- cannot passively diffuse across the membrane at a sufficient rate to electrically compensate this rapid movement of K^+-associated charge. The diffusion potential can be monitored and even calibrated using a variety of ΔΨ-dependent probes. For example, with the cationic membrane potential probe $DiOC_5(3)$, control PLs with KCl in/NaCl out display an obvious quench in probe fluorescence when valinomycin is added as the cationic probe accumulates inside in response to the generated negative inside ΔΨ (Figure 5 A, bottom trace, first arrow). An increase in fluorescence (return to intial baseline) is observed upon the subsequent addition of the K^+ and Na^+ ionophore gramicidin D (Figure 5A, bottom trace, second arrow) because Na^+ is now able to rapidly diffuse inward in response to the initial outward movement of K^+ and thereby collapse the electrical potential difference. A similar experiment wherein the same PLs are diluted into symmetrical KCl (Figure 5A, top trace) does not yield ΔΨ since there is no K^+ gradient driving outward K^+ diffusion.

Control PLs behaved as predicted under the conditions of this assay in either the presence (Figure 5A) or absence (Figure 5C) of 2 mM ATP. However, MDR−TCBD PLs with KCl inside and NaCl outside only form a diffusion potential upon addition of valinomycin in the presence of 2 mM ATP (Figure 5B). At 2 mM external ATP, the amplitude of the diffusion potential that is formed is similar to that formed by control PLs. However, in the absence of ATP, MDR−TCBD PLs no longer form a measurable diffusion potential upon addition of valinomycin (Figure 5D). In contrast, interestingly, when control and MDR−TCBD PLs are fabricated in the absence of Cl^- but diluted such that similar K^+ and Na^+ gradients exist prior to addition of valinomycin (i.e., potassium glutamate inside, sodium glutamate outside), diffusion potentials are formed for both in the absence of ATP (Figure 6C vs Figure 6D).

To further visualize this effect of ATP on diffusion potential, the experiments were repeated for both control and MDR−TCBD PLs in the presence of increasing amounts of ATP (Figure 7). While the ATP concentration did not affect the behavior of the control PLs (Figure 7A), increasing [ATP] clearly increased the magnitude of the potential generated by MDR−TCBD PLs (Figure 7B). At a concentration of

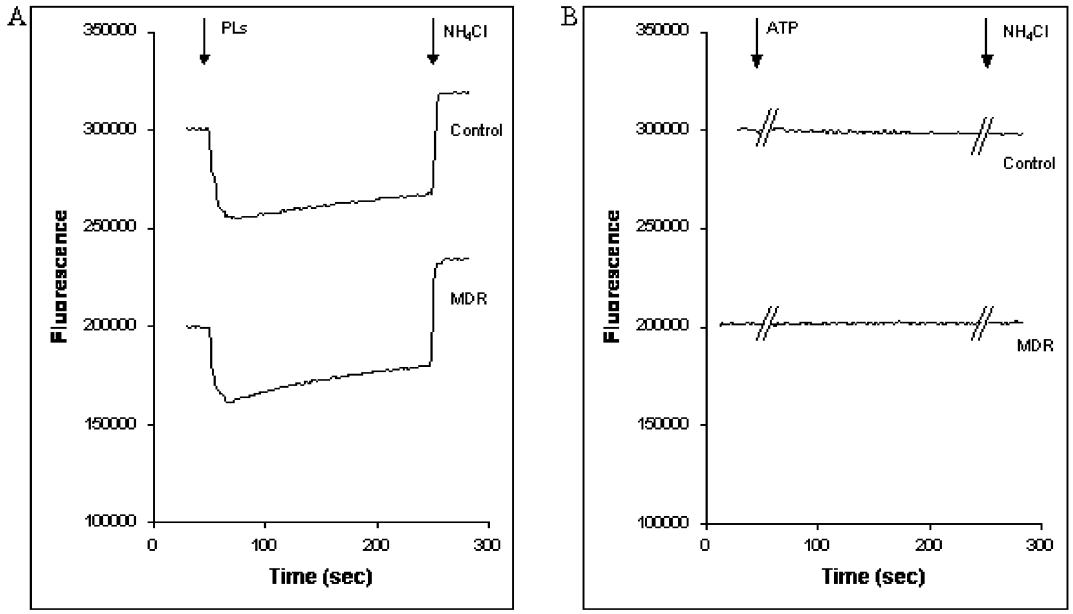

FIGURE 4: pH gradient formation assayed by acridine orange partitioning. (A) Control (top trace) or MDR−TCBD PLs (bottom trace) formed at pH 7.5 were diluted into buffer at pH 9.0 containing 2 μM AO to verify that the presence of a proton gradient (acid inside) could be monitored via AO quenching. The first arrow indicates addition of PLs, and the second arrow indicates the addition of 10 mM NH_4Cl to collapse the pH gradient. (B) Control (top) or MDR−TCBD (bottom trace) PLs formed at pH 7.5 in 140 mM KCl diluted as in (A) except the external pH was 7.5. Upon addition of ATP (first arrow) no measurable pH gradient was established under isotonic and symmetrical KCl conditions. Similar negative results were found with symmetrical potassium glutamate and symmetrical NaCl or in the presence of outward-directed Na^+ or Cl^- gradients (data not shown). Due to the practical limits of this assay, pH gradients of <0.5 unit are formally possible, but we have no evidence that pH gradients of appreciable magnitude are formed upon addition of ATP under any easily surveyed (see Figure 2) ionic conditions for MDR−TCBD PLs.

0.1 mM ATP, MDR−TCBD PLs displayed a potential that was approximately one-third of the potential formed by control PLs. In the presence of physiologic ATP (2 mM), the potential formed by MDR−TCBD PLs was similar to control. Addition of variable concentrations of ATP (up to 2 mM) did not affect the amplitude of the potential formed in the absence of Cl^- for either sample (data not shown).

To test that this effect is indeed due to hu MDR1 protein, the carbocyanine experiments were performed in the presence of hu MDR 1 inhibitors (Figure 8). While verapamil (VPL) did not affect control PLs (Figure 8A), it inhibited the MDR-mediated dissipation of ΔΨ in a dose-dependent manner (Figure 8B). In addition, 10 μM VPL stimulated ATPase activity for MDR−TCBD PLs as expected (not shown; see refs *13*, *16*, and *17*). Similarly, 4 μM cyclosporin A partially inhibited MDR−TCBD in the absence of ATP (not shown) but did not affect the control.

We also tested the effects of the nonhydrolyzable ATP analogue AMP-PNP and of cholesterol on membrane potential formation for MDR−TCBD PLs (Figure 9). In the presence of Cl^-, 2 mM AMP-PNP stimulated formation of a potential that was identical in magnitude to the potential stimulated by 2 mM ATP (Figure 9A), demonstrating that binding of nucleotide, but not hydrolysis, is necessary to close MDR−TCBD. When cholesterol was added to MDR−TCBD PLs in either the absence (top two traces, Figure 9B) or presence (bottom two traces, Figure 9B) of 2 mM ATP, the PLs appeared slightly "leaky", which could signify either modulation of ion transport by hu MDR 1 or altered diffusion of the carbocyanine probe. Nonetheless, in the absence of ATP, appreciable membrane potential was still not formed (top), and in the presence of cholesterol and ATP a potential of similar magnitude was formed initially (bottom). Thus, lipid composition may modulate hu MDR 1 activity as previously suggested (refs*5*, *8*, and *15* and references cited within), but cholesterol does not appreciably block apparent ion transport via hu MDR 1 in the absence of ATP (Figure 9B, top) or, in the presence of ATP, stimulate ion transport capable of competing with valinomycin-mediated K^+ transport (Figure 9B, bottom).

We next tested whether a flat response via the carbocyanine assay necessarily indicated a diffusion potential of zero. Since PLs have small internal volume, we suspected that low values of ΔΨ might be difficult to measure with this method. Indeed, a potential of <15−20 mV can exist for our PLs even if the carbocyanine response is essentially flat (not shown). However, greater ΔΨ is easily measured with our assay. Thus, in the presence of low levels of ATP, MDR−TCBD PLs are substantially depolarized, but they are not necessarily completely depolarized.

Calibration of ΔΨ *with Oxonol V.* To further quantify the depolarization effect, we adapted the JC-1 method employed for SUVs reconstituted with the K^+ channel (*23*). PLs reconstituted with 140 mM KCl inside were equilibrated with oxonol V in buffer containing 126 mM NaCl and 14 mM KCl in the presence and absence of 1 μM valinomycin. The valinomycin and 10-fold K^+ gradient clamps ΔΨ in control PLs to −60 mV. As increasing amounts of KCl are added, ΔΨ is clamped to lower values, and the fluorescent probe responds in a Nernstian fashion (Figure 10). As predicted from the carbocyanine experiments, in the presence of Cl^- and the absence of ATP MDR−TCBD PLs cannot hold the potential predicted by the Nernst equation (Figure 10B, solid squares). However, again as predicted by the carbocyanine assays, in the presence of 2 mM ATP (Figure 10B, solid triangles) or in the absence of Cl^- [substituting

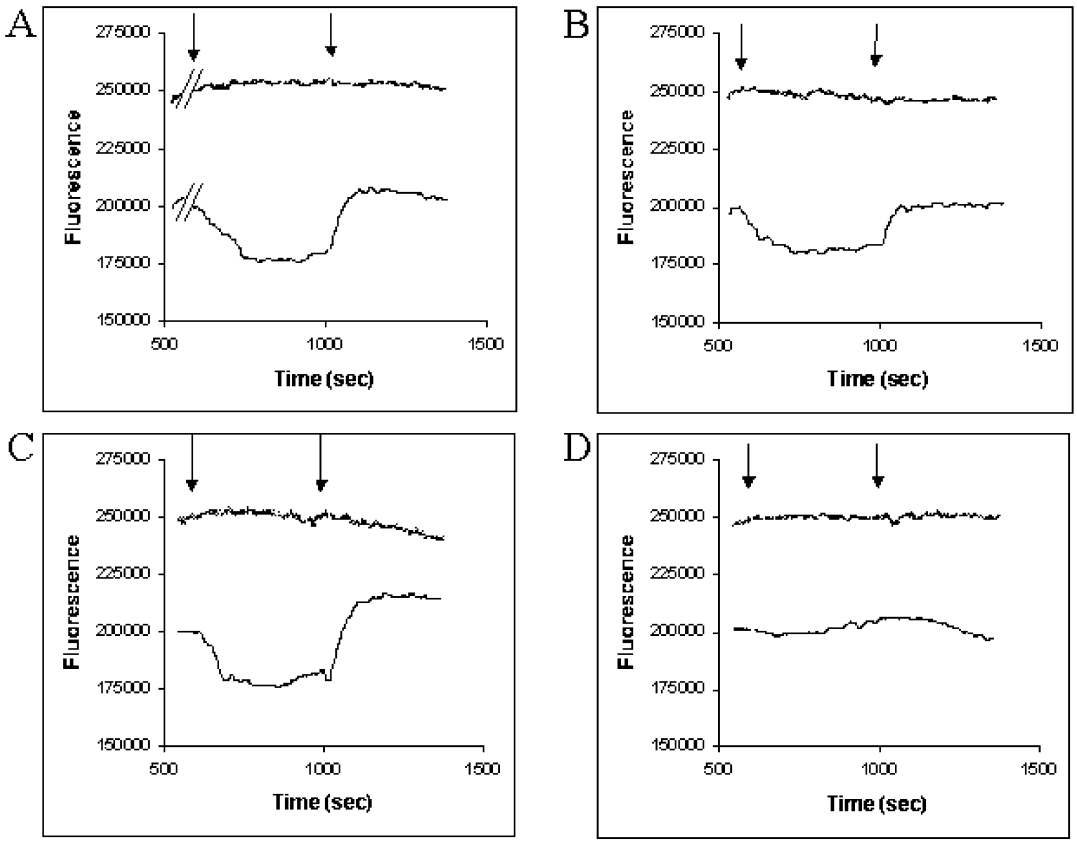

FIGURE 5: Membrane potential monitored by $DiOC_5(3)$. (A) The formation of a K^+/Na^+/valinomycin diffusion potential (see text) is easily observed in our PL preparations via monitoring the fluorescence of 0.1 μM $DiOC_5(3)$ (475 nm excitation, 496 nm emission). Control PLs reconstituted with KCl were diluted into KCl (A, top trace) or NaCl (A, bottom trace) buffer in the presence of 2 mM ATP. 7 μM valinomycin is added at the first arrow and 1.5 μM gramicidin D at the second. (B) The same experiments were repeated with MDR−TCBD PLs reconstituted with KCl and diluted in KCl (B, top trace) or NaCl (B, bottom trace). (C) The same experiments were repeated with the same control PLs in the absence of ATP. (D) The same experiments were repeated with the same MDR−TCBD PLs in the absence of ATP. Similar data were obtained in dozens of experiments with at least three PL preparations.

Cl^- with glutamate$^-$ (Figure 10C)] MDR−TCBD PLs behave similarly to controls. From calibrating the oxonol response at (predicted) −60 mV vs (predicted) 0 mV, the percent change in oxonol fluorescence for MDR−TCBD PLs in the presence of Cl^- and the absence of ATP is consistent with a potential of about −15 mV existing initially (i.e., conditions under which a −60 mV potential exists for control PLs). Thus, the carbocyanine assay (Figure 5D) does not necessarily illustrate a collapse of potential to zero for MDR−TCBD PLs + Cl^-/−ATP but a collapse to <-20 mV as measured by the oxonol calibration (Figure 10).

Since the partition coefficient (*P*) for valinomycin is approximately 7.5×10^3 (*27*), when the concentration in the transport buffer is 1 μM, the effective concentration in lipid is approximately 7.5 mM. As a K^+ carrier, the turnover number is 3×10^4 ions s^{-1} (molecule of valinomycin)$^{-1}$ (*27*). To effectively compete with valinomycin-mediated K^+ transport and thus manifest these depolarization effects, hu MDR 1 protein (approximately 1.25 μM in our experiments) would need to transport approximately 10^8 Cl^- ions s^{-1} (molecule of hu MDR 1)$^{-1}$. Such kinetics are consistent with ion channel function but not with carrier or pump function.

Formation of a Passive ΔpH. By forming a K^+/Na^+/valinomycin diffusion potential (negative inside) in control PLs, it is expected that a ΔpH (acid inside) will form simultaneously. As shown for control PLs reconstituted with potassium glutamate, pH 7.5 inside and diluted into buffer with sodium glutamate at pH 7.5, fluorescence of the ΔpH probe AO remains stable (Figure 11A, trace a), indicating no ΔpH. However, when the same experiment is performed with external buffer at pH 9.0 (Figure 11A, trace b) a ΔpH is easily observed. Upon addition of valinomycin at symmetrical pH (trace c, first arrow), a ΔpH forms secondary to the established ΔΨ. Performing the additive experiment wherein a 1.5 unit initial ΔpH plus a valinomycin-induced ΔΨ are present (trace d) produces an additive ΔpH as predicted (Figure 11A, trace d; that is, b + c = d). While the control PLs can hold this larger ΔpH for at least 200 s, MDR−TCBD PLs cannot hold ΔpH of this magnitude under conditions wherein an appreciable ΔΨ exists (Figure 11B, trace d). They can do so in the absence of ΔΨ (see Figure 4). That is, under these conditions (no Cl^-), where MDR−TCBD PLs do form a diffusion potential (see above), they become very leaky to H^+s. Not coincidentally, this is similar to one proposed scenario from a recent study showing increased rates of external cellular acidification due to hu MDR 1 (*28*).

DISCUSSION

An obvious general effect of exposing tumor cells to any of a variety of structurally diverse toxic anticancer drugs is a significant change in cellular metabolism. This typically includes significant changes in the utilization and synthesis of cellular ATP. Also, cells that become resistant to these

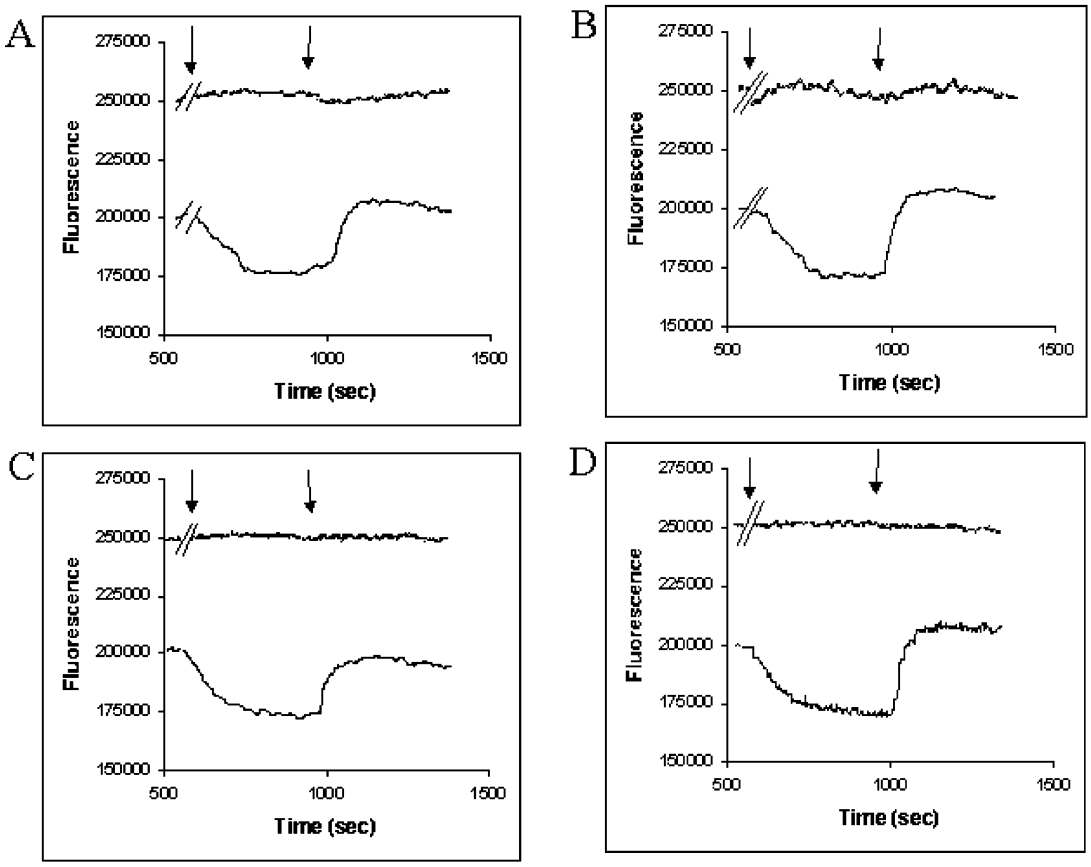

FIGURE 6: $DiOC_5(3)$ response is Cl^- dependent. (A) As in Figure 5 except control PLs reconstituted with potassium glutamate were diluted in KGlut (A, top) or NaGlut (A, bottom) buffer in the presence of 2 mM ATP. The addition of 7 μM valinomycin followed by the addition of 1.5 μM gramicidin D are again indicated with arrows. (B) The same experiments repeated with MDR−TCBD PLs reconstituted with KGlut and diluted in KGlut (B, top) or NaGlut (B, bottom) in the presence of 2 mM ATP. (C) The same experiments were repeated with control PLs in the absence of ATP, and in (D) the same MDR−TCBD PLs were diluted in the absence of ATP. MDR−TCBD PLs form membrane potential in the presence of Cl^- and presence of ATP (Figure 5B), in the presence or absence of ATP when Cl^- is absent (panels B and D) but not in the presence of Cl^- and absence of ATP (Figure 5D). Similar data were obtained in dozens of experiments with at least three PL preparations.

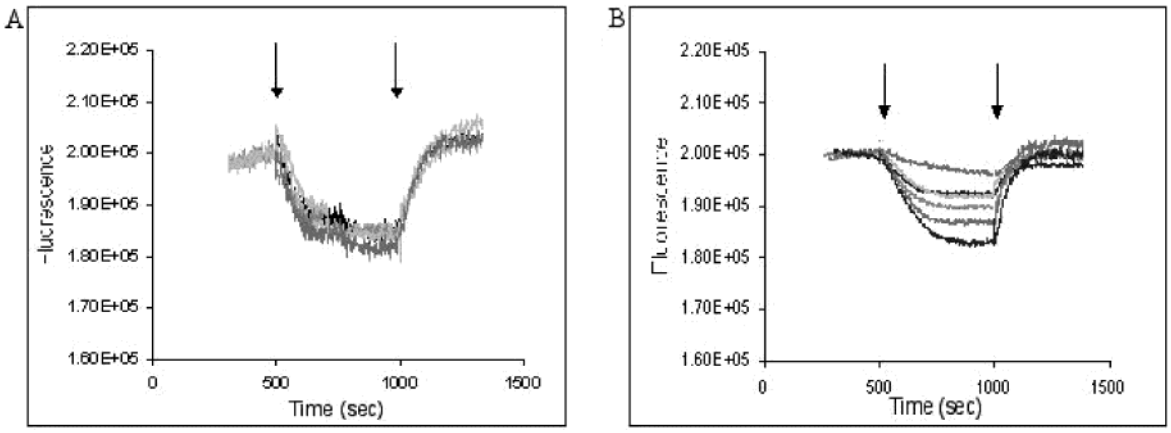

FIGURE 7: Membrane depolarization is ATP dependent. (A) Control and (B) MDR−TCBD PLs reconstituted in 140 mM KCl were diluted into isotonic buffer containing 140 mM NaCl containing increasing [ATP] (from the top: 0, 0.1, 0.2, 0.5, 1.0, and 2.0 mM). Valinomycin and gramicidin D were added at the arrows. At all concentrations of ATP, control PLs displayed membrane potential of similar magnitude. In contrast, MDR−TCBD PLs showed a steady loss of potential as [ATP] was decreased.

drugs over time almost always exhibit one or more significant perturbations in the signal transduction related to apoptosis, a process that normally culminates in dissipation of mitochondrial membrane potential and hence additional profound effects on cellular ATP. Drug-resistant cells also frequently exhibit overexpression of hu MDR 1 protein, which affords some level of protection against the repercussions of chemotherapeutic drug exposure. Although historically this defense has been envisioned to be via a mechanism that directly alters intracellular levels of the toxic drugs, it is now clear that this explanation is insufficient to explain all hu MDR 1-related resistance phenomena, some of which do not involve drugs at all (e.g., refs *1* and *2*). Hence, models wherein activation of protective hu MDR 1 function is linked

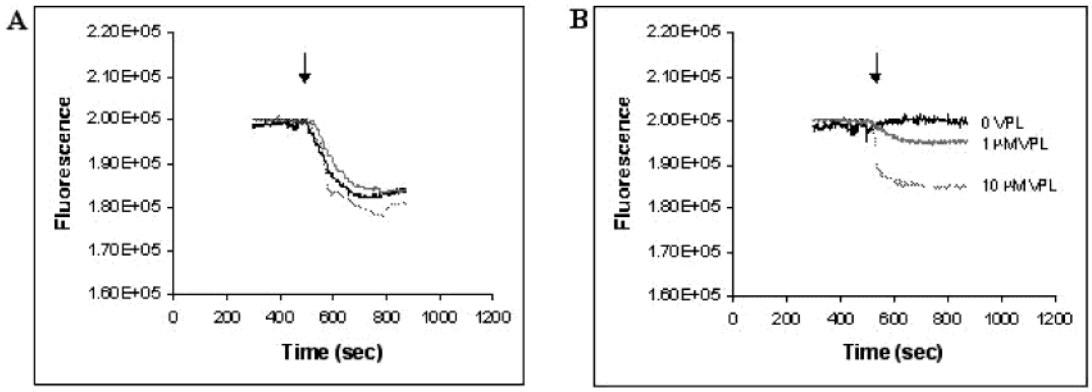

FIGURE 8: Verapamil (VPL) inhibits hu MDR 1. Control PLs (A) or MDR−TCBD PLs (B) reconstituted with KCl inside were diluted in transport buffer containing NaCl in the absence of ATP and (from top in each case) 0, 1, or 10 μM VPL. Formation of a membrane potential was monitored via $DiOC_5(3)$ fluorescence quenching as in Figure 5. The arrow indicates the addition of 1 μM valinomycin. Increasing [VPL] did not affect potential for the controls but increased the potential observed in MDR−TCBD PLs in a dose-dependent fashion.

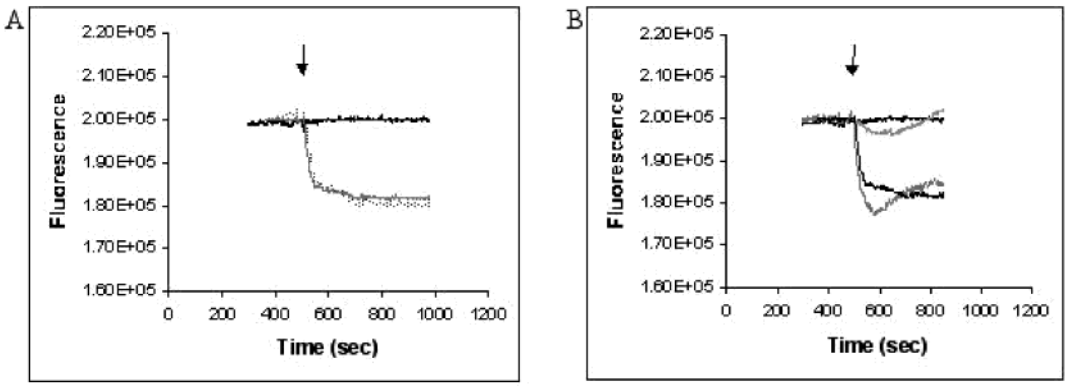

FIGURE 9: (A) 2 mM AMP-PNP (second trace from top) stimulates formation of membrane potential for MDR−TCBD PLs in the presence of Cl^- as well as does 2 mM ATP (third trace from the top). In the absence of nucleotide, the same PLs do not form a membrane potential (top trace). (B) Effect of 5% (weight percent of total lipid) cholesterol added to PLs formed by Racker sonification. Cholesterol was added to the purified *E. coli* lipid mixture via a concentrated stock made in chloroform. The top two traces are MDR−TCBD PLs minus ATP with KCl inside, and the bottom two are the same PL preparations plus 2 mM ATP (in both comparisons, the light trace is +cholesterol, and the dark trace is −cholesterol). In both (A) and (B), the K^+/Na^+/valinomycin diffusion potential is measured as in Figure 5.

in some other way to changes in ATP levels that accompany drug exposure or apoptosis are attractive. They offer a way to connect apoptotic signaling and metabolic effects linked to changes in ATP to the activation of hu MDR 1 and to thereby (in theory) explain facets of hu MDR 1 protection that clearly cannot be due to drug transport.

We find that, in the presence of relatively high levels of ATP, MDR−TCBD protein does not appear to pump a significant number of protons, nor does it appear to significantly affect generation of membrane potential by K^+/Na^+/valinomycin. However, as ATP is reduced, and in the presence of Cl^-, MDR−TCBD dissipates $\Delta\Psi$ caused by diffusion of K^+ in the presence of valinomycin. This dissipation is not reversed by addition of cholesterol but is reversed by verapamil and cyclosporin A (two compounds known to reverse the cellular effects of MDR protein at similar concentrations) in a dose-dependent fashion. In the absence of ATP, $\Delta\Psi$ is not dissipated to zero but to near −15 to −20 mV under conditions where control PLs easily hold potentials of −60 mV or greater. This effect is strikingly dependent on the concentration of ATP and the presence of Cl^-.

Some previous measurements of altered $\Delta\Psi$ caused by hu MDR 1 protein (e.g., ref *4*) have been challenged and suggested to perhaps be due to ATP-dependent "pumping" of the fluorescent probes used to monitor potential. In this study, the cationic carbocyanine probe is quenched as it diffuses into PLs in response to generation of a negative interior potential caused by valinomycin-induced outward diffusion of K^+ down its chemical gradient. We observe very little accumulation of probe (little diffusion inward) for the MDR−TCBD PLs in the complete *absence* of ATP. Loss of probe accumulation in the presence of inevitable diffusion of K^+ via valinomycin cannot be explained by outward pumping of the probe, since ATP (the energy source for the suggested probe-pumping process) is absent.

Regulation of $\Delta\Psi$ is connected to a number of cell biological phenomena. The most well studied examples are signal transduction in muscle cells and neurons, but changes in $\Delta\Psi$ for other cell types directly affect passive diffusion of charged drugs, the efficiency of complement-mediated cytotoxicity, regulation of cytosolic pH, regulation of apoptosis, and other phenomena that have been observed in drug-resistant tumor cells overexpressing hu MDR 1 protein (*7*). Reported observations of $\Delta\Psi$ perturbations due to hu MDR 1 overexpression have been controversial, but much of this controversy is likely due to the variety of very complex model systems that have been inspected. To our knowledge, only two reports have examined $\Delta\Psi$ for "true" hu MDR 1 transfectants created without any exposure to chemotherapeutic drugs that are known to cause a variety of epiphenomena. One (*4*) clearly showed that $\Delta\Psi$ was depolarized

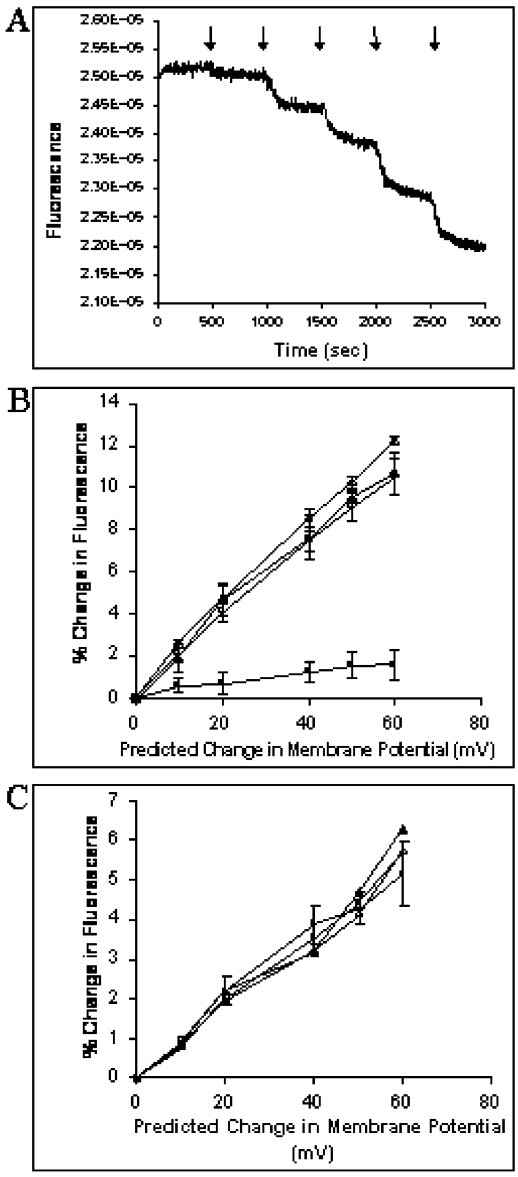

FIGURE 10: Calibration of membrane potential with oxonol V. (A) Control PLs reconstituted with 140 mM KCl were equilibrated with 8 μM oxonol V, 126 mM NaCl, and 14 mM KCl ± 1 μM valinomycin. Each arrow corresponds to the addition of KCl such that the final external concentration was 19.6, 29.4, 64.4, 95.2, and 140 mM, respectively. Shown is the difference between the experiment done in the presence vs absence of valinomycin. (B) The experiment described in (A) was repeated at least three times with control (open symbols) and MDR−TCBD (closed symbols) PLs in either the presence (triangles) or absence (squares) of 2 mM ATP. The percent change in fluorescence upon each addition of KCl was plotted vs the calculated change in ΔΨ computed via the Nernst equation. (C) Same as (B) except PLs were reconstituted with potassium glutamate and glutamate salts outside. When Cl^- was no longer present, MDR−TCBD PLs behaved identically to controls, whereas in the presence of Cl^- and the absence of ATP (panel B, closed squares) a much smaller change in ΔΨ (approximately 15 mV) was measured. Thus, we estimate that under conditions where control PLs maintain −60 mV potential (and under conditions where MDR−TCBD PLs in the presence of ATP maintain −60 mV potential), MDR−TCBD PLs in the absence of ATP are only able to maintain potentials approximately one-fourth as large. Knowing the concentration of valinomycin, its lipid partitioning coefficient, the rate at which it catalyzes K^+ diffusion down a 10-fold concentration gradient, and the [MDR−TCBD] in these PLs, the results are consistent with MDR−TCBD protein functioning as a Cl^- channel in the presence of membrane potential and at low [ATP].

in fibroblasts expressing high levels of hu MDR 1. Another study (*5*) argued that hu MDR 1 overexpression did not change ΔΨ but might perturb intramembranous potential (*29*). However, in this study a possibly hu MDR 1-specific ΔΨ depolarization was indeed seen when ATP was eliminated from the pipet used to measure ΔΨ, but the data were not of sufficiently low statistical deviation to make the conclusion unequivocal. Nonetheless, the potential correspondence between these previous results and those presented in this paper is intriguing, as are other facets of what we observe.

Via the simplest molecular model that can be generated from these data, purified hu MDR 1 protein performs passive Cl^- transport in the presence of significant (≥ −60 mV) ΔΨ and in the presence of relatively low concentrations of ATP. This passive Cl^- movement acts to dissipate ΔΨ dominated by K^+ flux. A variety of additional extensive studies are needed to determine precisely how loss of ATP stimulates the apparent Cl^- conductance. Also, we note that, topologically, MDR−TCBD protein is oriented primarily "inside out" while the membrane potential formed for the PLs is negative inside. This means that MDR−TCBD is exposed to a membrane potential of opposite polarity relative to the situation that is expected for MDR protein within a cell plasma membrane. Most voltage-regulated ion channels conduct ions under either polarity but typically have higher current for one polarity vs the other. More detailed studies with these and other model systems should eventually quantify the precise current/voltage relationship for apparent Cl^- permeability via MDR protein.

We also note that these studies are performed with a hu MDR 1 biotin acceptor domain fusion protein. Although we feel it is highly unlikely based on ATPase and VPL data, formally, it is possible that the TCBD domain influences the function of hu MDR 1 or that it might even promote "carryover" of some trace contaminant during purification that is not visible on our gels.

Regardless, our ATP-regulated Cl^- transport model connects to previous well-known but controversial Cl^- channel hypotheses for hu MDR 1 in rather interesting ways. That is, many previous electrophysiological studies examining putative ion transport via hu MDR 1 protein reported unusual Cl^- transport in cells with hu MDR 1 vs without hu MDR 1, but other studies were unable to reproduce this result (*9*, *30*). In the studies that reported Cl^- transport via hu MDR 1 [either direct transport or perhaps stimulation of an endogeneous Cl^- transporter in phosphorylation-dependent fashion (*31*)], the method used to elicit the measured Cl^- conductance was, invariably, hypotonic shock. Perhaps not coincidentally, hypotonic shock drops cellular ATP levels, but in a cell-specific fashion (*32*, *33*). Studies that failed to observe conductance invariably kept constant (and relatively high) levels of ATP fixed within the pipet used in the electrophysiologic experiments. For example, one study that did not observe Cl^- conductance maintained constant 4 mM ATP in the pipet (*34*); hence similar high [ATP] would be within the cell expressing hu MDR 1 at all times.

There is some homology between hu MDR 1 and prokaryotic transporters implicated in small molecule solute transport; however, two perhaps more relevant homologues of hu MDR 1 are the hu CFTR and hu SUR ion channels. Perhaps not coincidentally, ion transport by both is regulated

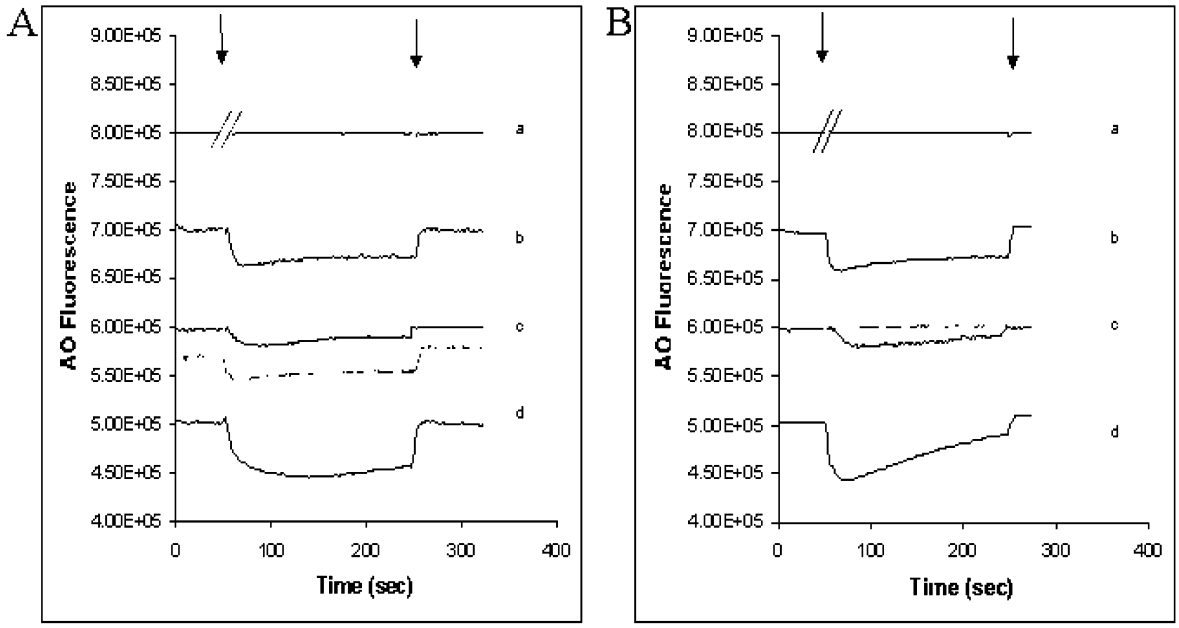

FIGURE 11: Passive ΔpH. Control (A) or MDR−TCBD (B) PLs reconstituted with 140 mM potassium glutamate, pH 7.5, were diluted into isotonic buffer containing acridine orange and 140 mM sodium glutamate at pH 7.5 (top trace of each panel, labeled a), at pH 9.0 (second trace, b), pH 7.5 + 1 μM valinomycin (trace c, solid line), or pH 9.0 + 1 μM valinomycin (trace d). Also shown (trace c, dashed line) is the symmetrical pH experiment plus 1 μM valinomycin but using KCl and NaCl salts. The presence of a ΔpH (trace b) is easily distinguished from the absence (trace a). Also, the presence of a K^+/Na^+/valinomycin diffusion potential stimulates passive H^+ movement (trace c, solid line) as expected. Since the baseline for this ΔpH looked less flat for MDR−TCBD PLs vs control (compare panel A, trace c, solid, to panel B, trace c, solid trace), we repeated experiment c under conditions where a larger ΔpH would be present (e.g., trace d). Under these conditions, control PLs stably held the ΔpH (in the presence of membrane potential), whereas MDR−TCBD PLs were conspicuously leaky. In the absence of ΔΨ but the presence of a similar magnitude of ΔpH (e.g., see Figure 4A, bottom trace) MDR−TCBD PLs do not leak H^+. We suggest that, in the presence of a ΔΨ, MDR protein allows the passive movement of H^+ down its concentration gradient.

by ATP binding and ATP hydrolysis, but in different ways for each channel. Monomeric CFTR functions as an ATP-dependent Cl^- channel (*35*), whereas SUR appears to function as a multimeric complex with K_{ir} proteins to form an ATP-gated K^+ channel (*36*). In the case of CFTR, ATP positively regulates channel activity, whereas depletion of ATP activates the SUR. ATP regulation of SUR/K_{ir} channel complexes is complex, with ATP binding at both K_{ir} and SUR subunits apparently involved. Regardless, these examples show that ATP can regulate ion transport by ABC proteins in both positive and negative fashion. The point is, although perhaps initially surprising, the model we propose is entirely consistent with the very well studied behavior of close hu MDR 1 homologues, as well as earlier Cl^- channel observations promoted by hypotonicity.

It is not entirely clear to us what role putative hu MDR 1 mediated Cl^- conductance promoted by reduced [ATP] might play in cell physiology, but perhaps this transport represents a "partner" to ubiquitous ATP depletion stimulated K^+ conductance in instances where cell volume regulation is imperative. For example, cells induced to apoptose show reduced cellular ATP and pronounced cell volume changes. In cells attempting to avoid apoptotic signaling (i.e., cells that have developed chemotherapeutic drug resistance), the presence of hu MDR 1 might help to modify the cell volume or cell pH changes that are normally initiated at the beginning of the apoptotic cascade. Indeed, such a possibility is consistent with previous work that examined delayed apoptosis in hu MDR 1 overexpressing transfectants (*1*) as well as altered volume regulation by hu MDR 1 (*10*).

In summary, biotinylated hu MDR 1 protein was purified and reconstituted in fully functional form. ATPase activity exhibited the same pH dependency as has been measured previously (*16*), and specific activity was similar to other reports of very active purified MDR protein. ATP hydrolysis was not accompanied by measurable H^+ pumping for PLs under the conditions of our assay. However, MDR−TCBD protein has clear and significant Cl^-- and ATP-dependent effects on ΔΨ formed by the inevitable passive diffusion of K^+ via valinomycin in the presence of a K^+ gradient. These effects are inhibited by VPL and CsA and may be further influenced by lipid composition (e.g., cholesterol content). More detailed analysis of lipid composition effects is warranted. Finally, under conditions that mimic those at which there is optimum collapse of ΔΨ via hu MDR 1, we also note a passive transport of H^+ down its concentration gradient. This result may help to further elucidate other recent results showing faster rates of extracellular acidification for hu MDR 1 overexpressing cells (*28*) and, along with membrane potential effects, help to explain altered leaflet disposition of some lipids via MDR proteins (e.g., refs *8* and *9* and references cited within).

ACKNOWLEDGMENT

We thank Drs. A. Tzagoloff (Columbia University) and R. Wadkins (Johns Hopkins University) for plasmid YEp352/BIO6 and helpful discussions, respectively, and our laboratory colleagues V. Ovchinnikov, H. Zhang, L. M. B. Ursos, T. N. Bennett, S. Freitas, S. Dzekunov, and C. T. Santai for experimental help.

REFERENCES

1. Robinson, L. J., Roberts, W. K., Ling, T. T., Lamming, D., Sternberg, S. S., and Roepe, P. D. (1997) Human MDR 1 protein overexpression delays the apoptotic cascade in Chinese hamster ovary fibroblasts, *Biochemistry 36*, 11169−11178.
2. Weisburg, J. H., Curcio, M., Caron, P. C., Raghu, G., Mechetner, E. B., Roepe, P. D., and Scheinberg, D. A. (1996) The multidrug resistance phenotype confers immunological resistance, *J. Exp. Med. 183*, 2699−2704.
3. Weisburg, J. H., Roepe, P. D., Dzekunov, S., and Scheinberg, D. A. (1999) Intracellular pH and multidrug resistance regulate complement-mediated cytotoxicity of nucleated human cells, *J. Biol. Chem. 274*, 10877−10888.
4. Hoffman, M. M., Wei, L.-Y., and Roepe, P. D. (1996) Are altered pH_i and membrane potential in hu MDR1 transfectants sufficient to cause MDR protein-mediated multidrug resistance?, *J. Gen. Physiol. 108*, 295−313.
5. Luker, G. D., Flagg, T. P., Sha, Q., Luker, K. E., Pica, C. M., Nichols, C. G., and Piwnica-Worms, D. (2001) *MDR1* P-glycoprotein Reduces Influx of Substrates without Affecting Membrane Potential, *J. Biol. Chem. 276*, 49053−49060.
6. Gill, D. R., Hyde, S. C., Higgins, C. F., Valverde, M. A., Mintenig, G. M., and Sepulveda, F. V. (1992) Separation of drug transport and chloride channel functions of the human multidrug resistance P-glycoprotein, *Cell 71*, 23−32.
7. Roepe, P. D. (2000) What is the Precise Role of Human MDR 1 Protein in Chemotherapeutic Drug Resistance?, *Curr. Pharm. Des. 6*, 241−260.
8. Smith, A. J., Timmermans-Hereijgers, J. L., Roelofsen, B., Wirtz, K. W., van Blitterswijk, W. J., Smit, J. J., Schinkel, A. H., and Borst, P. (1994) The human MDR3 P-glycoprotein promotes translocation of phosphatidylcholine through the plasma membrane of fibroblasts from transgenic mice, *FEBS Lett. 354*, 263−266.
9. Bond, T. D., Higgins, C. F., and Valverde, M. A. (1998) P-glycoprotein and swelling-activated chloride channels, *Methods Enzymol. 292*, 359−370.
10. Hoffman, M. M., and Roepe, P. D. (1997) Analysis of ion transport perturbations caused by hu MDR1 protein overexpression, *Biochemistry 36*, 11153−11168.
11. Roepe, P. D., Wei, L. Y., Cruz, J., and Carlson, D. (1993) Lower electrical membrane potential and altered pH_i homeostasis in multidrug-resistant (MDR) cells: further characterization of a series of MDR cell lines expressing different levels of P-glycoprotein, *Biochemistry 32*, 11042−11056.
12. Matsuyama, S., Llopis, J., Deveraux, O. L., Tsien, R. Y., and Reed, J. C. (2000) Changes in intramitochondrial and cytosolic pH: early events that modulate caspase activation during apoptosis, *Nat. Cell Biol. 2*, 318−325.
13. Julien, M., Kajiji, S., Kaback, H. R., and Gros, P. (2000) Simple Purification of Highly Active Biotinylated P-Glycoprotein: Enantiomer-Specific Modulation of Drug-Stimulated ATPase Activity, *Biochemistry 39*, 75−85.
14. Mao, Q., and Scarborough, G. A. (1997) Purification of Functional Human P-glycoprotein Expressed in *Saccharomyces cerevisiae*, *Biochim. Biophys. Acta 1327*, 107−118.
15. Callaghan, R., Berridge, G., Ferry, D. R., and Higgins, C. F. (1997) The Functional Purification of P-glycoprotein is Dependent on Maintenance of a Lipid−Protein Interface, *Biochim. Biophys. Acta 1328*, 109−124.
16. Urbatsch, I. L., Al-Shawi, M. K., and Senior, A. E. (1994) Characterization of the ATPase Activity of Purified Chinese Hamster P-glycoprotein, *Biochemistry 33*, 7069−7076.
17. Shapiro, A. B., and Ling, V. (1994) ATPase Activity of Purified and Reconstituted P-glycoprotein from Chinese Hamster Ovary Cells, *J. Biol. Chem. 269*, 3745−3754.
18. Urbatsch, I. L., Beaudet, L., Carrier, I., and Gros, P. (1998) Mutations in Either Nucleotide Binding Site of P-glycoprotein (Mdr3) Prevent Vanadate Trapping of Nucleotide at Both Sites, *Biochemistry 37*, 4592−4602.
19. Loo, T. W., and Clarke, D. M. (1995) Rapid Purification of Human P-glycoprotein Mutants Expressed Transiently in HEK 293 Cells by Nickel−Chelate Chromatography and Characterization of their Drug-Stimulated ATPase Activities, *J. Biol. Chem. 270*, 21449−21452.
20. Goffeau, A., and Dufour, J.-P. (1988) Plasma Membrane ATPase from the Yeast *Saccharomyces cerevisiae*, *Methods Enzymol. 157*, 528−533.
21. Fritz, F., Howard, E. M., Hoffman, M. M., and Roepe, P. D. (1999) Evidence for Altered Ion Transport in *Saccharomyces cerevisiae* Overexpressing Human MDR 1 Protein, *Biochemistry 38*, 4214−4226.
22. Chifflet, S., Torriglia, A., Chiesa, R., and Tolosa, S. (1988) A method for the determination of inorganic phosphate in the presence of labile organic phosphate and high concentrations of protein: application to lens ATPases, *Anal. Biochem. 168*, 1−4.
23. Chanda, B., and Mathew, M. K. (1999) Functional Reconstitution of Bacterially Expressed Human Potassium Channels in Proteoliposomes: Membrane Potential Measurements with JC-1 to Assay Ion Channel Activity, *Biochim. Biophys. Acta 1416*, 92−100.
24. Sharom, F. J., Yu, X., Chu, J. W., and Doige, C. A. (1995) Characterization of the ATPase Activity of P-glycoprotein from multidrug resistant Chinese hamster ovary cells, *Biochem. J. 308*, 381−390.
25. Figler, R. A., Omote, H., Nakamoto, R. K., and Al-Shawi, M. K. (2000) Use of chemical chaperones in the yeast *Saccharomyces cerevisiae* to enhance heterologous membrane protein expression: high-yield expression and purification of human P-glycoprotein, *Arch. Biochem. Biophys. 376*, 34−46.
26. Santai, C. T., Fritz, F., and Roepe, P. D. (1999) Effects of Ion Gradients on H^+ Transport Mediated by Human MDR 1 Protein, *Biochemistry 38*, 4227−4234.
27. Benz, R., and Lauger, P. (1976) Kinetic analysis of carrier-mediated ion transport by the charge-pulse technique, *J. Membr. Biol. 27*, 171−191.
28. Landwojtowicz, E., Nervi, P., and Seelig, A. (2002) Real-time monitoring of P-glycoprotein activation in living cells, *Biochemistry 41*, 8050−8057.
29. Clarke, R. J., and Lüpfert, C. (1999) Influence of anions and cations on the dipole potential of phosphatidylcholine vesicles: a basis for the Hofmeister Effect, *Biophys. J. 76*, 2614−2624.
30. Idriss, H. T., Hannun, Y. A., Boulpaep, E., and Basavappa, S. (2000) Regulation of volume-activated chloride channels by P-glycoprotein: phosphorylation has the final say!, *J. Physiol. 5243*, 629−636.
31. Hardy, S. P., Goodfellow, H. R., Valverde, M. A., Gill, D. R., Sepulveda, V., and Higgins, C. F. (1995) Protein kinase C-mediated phosphorylation of the human multidrug resistance P-glycoprotein regulates cell volume-activated chloride channels, *EMBO J. 14*, 68−75.
32. Van der Wijk, T., de Jonge, H. R., and Tilly, B. C. (1999) Osmotic swelling-induced ATP release mediates the activation of extracellular signal-regulated protein kinase (Erk)-1/2 but not the activation of osmo-sensitive anion channels, *Biochem. J. 343*, 579−586.
33. Mitchell, C. H. (2001) Release of ATP by human retinal pigment epithelial cell line: potential for autocrine stimulation through sub retinal space, *J. Physiol. 534*, 193−202.
34. Viana, F., Van Acker, K., De Greef, C., Eggermont, J., Raeymaekers, L., Droogmans, G., and Nilius, B. (1995) Drug-transport and volume-activated chloride channel functions in human erythroleukemia cells: relation to expression level of P-glycoprotein, *J. Membr. Biol. 145*, 87−98.
35. Gadsby, D. C., and Nairn, A. C. (1999) Control of CFTR channel gating by phosphorylation and nucleotide hydrolysis, *Physiol. Rev. 79*, S77−S107.
36. Baukrowitz, T., and Fakler, B. (2000) KATP channels gated by intracellular nucleotides and phospholipids, *Eur. J. Biochem. 267*, 5842−5848.

BI026706I